Int. J. Solids Structures, 1975, Vol. 11, pp. 521–538. Pergamon Press. Printed in Great Britain

THE STRESS FIELD IN THE NEIGHBORHOOD OF A BRANCHED CRACK IN AN INFINITE ELASTIC SHEET†

SAILENDRA N. CHATTERJEE‡
Department of Mechanical Engineering, Indian Institute of Science, Bangalore-12, India

(*Received* 13 *March* 1974; *revised* 29 *May* 1974)

Abstract—The problem of a branched crack consisting of a main crack and a straight branch starting from one of its tip located in an infinite elastic sheet is considered under the assumptions of two-dimensional theory of Elasticity. Employing Kolosov-Muskhelishvili representation of the stress function and other well known techniques the problem is reduced to the solution of an integral equation. The nature of the stress singularity at the re-entrant corner, where the two branches of the crack meet, is discussed. Based upon a numerical solution of the integral equation the stress intensity factors at the two tips are computed for two types of prescribed traction at infinity and various geometric configurations of the branched crack.

1. INTRODUCTION

In brittle or quasi-brittle type of fracture, crack extension is often found to occur in directions different from the plane containing the crack. These extensions are usually called branches and several such branches may develop from the tip of a crack propagating at certain velocities [1, 2]. A slow process of crack branching of the type shown in Fig. 1 is observed during quasi-static loading of brittle materials under bi-axial compression. This type of crack growth has been explained (see Ref. [3], pp. 426–440) by a proper interpretation of the criterion of failure due to Griffith [4] who considered randomly oriented elliptical flaws and proposed that fracture will occur when the maximum tensile stress at the edge of one of the flaws reaches a critical value.

The Griffith–Irwin–Barenblatt hypothesis for crack instability successfully predicts the critical tensile stress for a crack of given length in an isotropic material when the deformations near the crack tip are of the opening mode or mode I type and under such conditions the crack extends in its own plane. However, a combination of mode I and mode II type of deformations or a pure mode II behaviour may cause development of branching cracks as shown in Fig. 1 [5]. Such cracks are also found to occur in the stressing of anisotropic materials.

Although the phenomenon of crack branching is interesting and of great importance in fracture mechanics, because of the mathematical complexity of the problem, very few attempts have been made to investigate the nature of the stress field near a bifurcated crack. In this study we consider a branched crack with two straight arms in an infinite sheet as shown in Fig. 2. It consists of a main crack and a branch starting from one of its tip and is simpler than the crack configuration shown in Fig. 1 from the view point of mathematical formulation. However, the stress fields near the tip of the branch for the two crack configurations will be almost identical if the length of the branch is small compared to that of the main crack. The two arms of the crack configuration (Fig. 2) are of finite length and therefore, the stress field near each tip can be characterized by the two stress intensity factors K_I and K_{II}.

By the use of the Kolsov–Muskhelishvili representation [6] of the biharmonic stress function, a mapping function due to Darwin [7] as well as an extension principle, the two-dimensional

†A major part of this work was completed when the author was a NRC Resident Research Associate at the Army Materials and Mechanics Research Center, Watertown, MA 02172, U.S.A.

‡At present with Mat. Sci. Corpn., Blue Bell office Campus, Blue Bell, PA 19422, U.S.A.

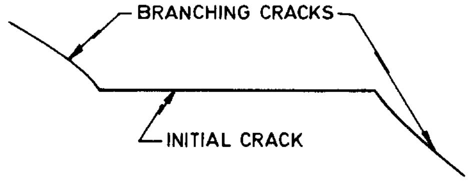

Fig. 1. Branching cracks.

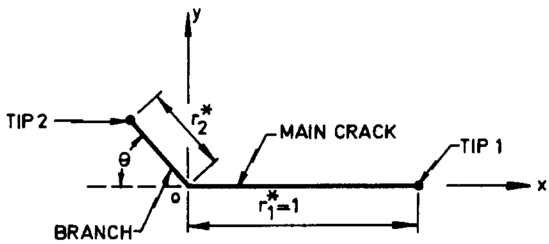

Fig. 2. Branched crack with two arms.

elasticity problem under consideration is reduced to the determination of a sectionally holomorphic function $\eta(\zeta)$. The solution is expressed in the form of a Cauchy integral over the line of discontinuity involving an unknown complex valued function which has to be determined by solving an integral equation. The kernel of the equation is singular at the two end points, which correspond to the junction of the two arms of the crack in the z-plane. This is a characteristic of the non-holomorphic nature of the function $\eta(\zeta)$ at these two points. It is shown that the solution $\eta(\zeta)$ yields the well known stress singularity at the re-entrant corner[8]. The integral equation is numerically solved and the stress intensity factors are obtained for two types of prescribed tractions at infinity and various geometric configurations of the branched crack. No attempt is made here to propose any criterion for the development of branching cracks or their extension.

It should be noted that the crack configuration shown in Fig. 2 was also considered by Hussain *et al.*[9]. Their aim was to obtain the limiting value of the strain energy release rate at the tip of the branch when its length approaches zero. Based on the hypothesis that the branch will develop in a direction in which this limiting value is a maximum they proposed a criterion of crack instability for mixed mode loading conditions. The work[9] also contains the results of an experimental investigation with a crack tip under a state of mode II type of deformation. The proposed criterion is found to be in better agreement with the experimental results than the "Maximum Stress" concept[4, 5, 10].

Andersson[11] attempted to obtain the stress intensity factors at the tips of a star-shaped contour and we have made use of some of his results here. Andersson's formulation however, contains an error[12] due to which his results and conclusions are not reliable, although it has been suggested that they are good when the lengths of the branches are small compared to that of the main crack.

2. FORMULATION OF THE PROBLEM

We consider a branched crack in an infinite sheet and introduce the co-ordinates x, y as shown in Fig. 2. The length of the main crack is taken to be unity ($r_1^* = 1$). The branch is of length r_2^* and it makes an angle $\pi-\theta$ with the x-axis. Use will be made of the following mapping function due to

Darwin[7] to transform the crack contour and its exterior onto the region $|\zeta| \geq 1$ (see Fig. 3).

$$z = x + iy = \omega(\zeta) = A\zeta^{-1}(\zeta - e^{i\alpha_1})^{\lambda_1}(\zeta - e^{i\alpha_2})^{\lambda_2} \tag{1}$$

where

$$\begin{aligned} \pi\lambda_1 &= \pi - \theta \\ \pi\lambda_2 &= \pi + \theta \end{aligned} \tag{2}$$

and A is a real constant.

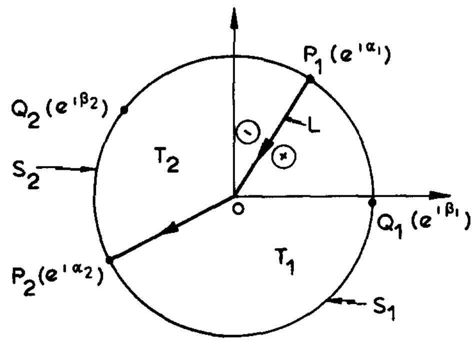

Fig. 3. Branched crack transformed onto the unit circle in ζ-plane.

The circle $|\zeta| = 1$ corresponds to the crack contour. The points $P_j(\zeta = e^{i\alpha_j};\ j = 1, 2)$ both correspond to the origin in the z plane. $\omega(e^{i\alpha_1})$ and $\omega(e^{i\alpha_2})$ however, lie on the upper and lower faces of the main crack, respectively. Points $Q_j(\zeta = e^{i\beta_j};\ j = 1, 2)$ correspond to the crack tips 1 and 2. The constant A in equation (1), α_1, α_2, β_1 and β_2 are obtained by solving the following system of equations (see Ref. [11]).

$$\alpha_1\lambda_1 + \alpha_2\lambda_2 = 2\pi \tag{3}$$

$$\sum_{k=1}^{2} \lambda_k \cot\left(\frac{\alpha_k - \beta_l}{2}\right) = 0; \qquad l = 1, 2 \tag{4}$$

$$4A \prod_{k=1}^{2} \left| \sin\left(\frac{\beta_l - \alpha_k}{2}\right)\right|^{\lambda_k} = r_l^*; \qquad l = 1, 2 \tag{5}$$

Equation (3) has been obtained by demanding that the point $\zeta = 1$ corresponds to a point on the surface of the main crack, i.e. $\arg(\omega(1)) = 0$. Consequently the arc $P_2Q_1P_1(S_1)$ of the circle $|\zeta| = 1$ maps onto the main crack and the arc $P_1Q_2P_2(S_2)$ corresponds to the two surfaces of the branch. The set of equations (3–5) was solved for various values of θ and r_2^* with the help of an iterative scheme.

It is clear that the mapping function $\omega(\zeta)$ has two branch points P_1 and P_2 and the branch cut may be chosen as any line joining P_1 and P_2 inside or on the unit circle. Here we will assume that the cut lies inside the circle (say the line P_1OP_2 or the straight line P_1P_2).

Complex representation. Following Muskhelishvili [6] we introduce the two functions $\phi(\zeta)$ and $\psi(\zeta)$ holomorphic outside the unit circle except at the point at infinity such that

$$\sigma_x + \sigma_y = 4R\,e\{\phi'(\zeta)/\omega'(\zeta)\} \tag{6}$$

$$\sigma_y - \sigma_x + 2i\tau_{xy} = 2\{\overline{\omega(\zeta)}[\phi'(\zeta)/\omega'(\zeta)]' + \psi'(\zeta)\}/\omega'(\zeta).$$

Since the crack surfaces are free of stresses we have for $\zeta = t = e^{iq}$; $0 \leq q \leq 2\pi$,

$$\phi(t) + \frac{\omega(t)}{\overline{\omega'(t)}}\overline{\phi'(t)} + \overline{\psi(t)} = 0 \tag{7}$$

The quantity $\dfrac{\omega(t)}{\overline{\omega'(t)}}$ can be written as

$$\frac{\omega(t)}{\overline{\omega'(t)}} = \frac{\omega(t)}{\overline{\omega(t)}}\left\{\overline{\frac{\omega(t)}{\omega'(t)}}\right\} = -\frac{\omega(t)}{\overline{\omega(t)}} \cdot \frac{1}{\overline{tg(t)}} \tag{8}$$

where

$$g(t) = 1 + \frac{\lambda_1 e^{i\alpha_1}}{t - e^{i\alpha_1}} + \frac{\lambda_2 e^{i\alpha_2}}{t - e^{i\alpha_2}} \tag{9a}$$

$$= \frac{(t - e^{i\beta_1})(t - e^{i\beta_2})}{(t - e^{i\alpha_1})(t - e^{i\alpha_2})} \tag{9b}$$

and

$$\begin{aligned} \frac{\omega(t)}{\overline{\omega(t)}} &= K_1 = 1; \quad 0 \leq \arg(t) = q < \alpha_1 \\ &\qquad \alpha_2 < q \leq 2\pi \\ &\qquad (t \text{ lies on } S_1 = P_2Q_1P_1) \\ &= K_2 = e^{-2i\theta}; \quad \alpha_1 < q < \alpha_2 \\ &\qquad (t \text{ lies on } S_2 = P_1Q_2P_2). \end{aligned} \tag{10}$$

Equation (9b) follows from (9a) since the zeroes of $g(t)$ should be the same as those of $\omega'(t)$. In view of (8–10) equation (7) can be written as

$$t\phi(t) - \frac{K_m}{\overline{g(t)}}\overline{\phi'(t)} + \overline{t\psi(t)} = 0; \qquad t \text{ lies on } S_m, \qquad m = 1,2. \tag{11}$$

Denoting the regions $P_2OP_1Q_1$ by T_1 and $P_2OP_1Q_2$ by T_2 (see Fig. 3), the definition of $\phi(\zeta)$, originally defined outside the unit circle, is extended to the regions T_1 and T_2 by writing

$$\begin{aligned} \eta(\zeta) = \zeta\phi(\zeta) &= \frac{K_m}{\bar{g}(\zeta)}\bar{\phi}'(1/\zeta) - \zeta\bar{\psi}(1/\zeta); \\ &\zeta \text{ lies in } T_m; \qquad m = 1,2 \end{aligned} \tag{12a}$$

where

$$\bar{f}(1/\zeta) = \overline{f(1/\bar{\zeta})}. \tag{12b}$$

Since $K_1 \neq K_2$, the function $\eta(\zeta)$ is discontinuous across the piecewise smooth line $L = P_1OP_2$. If the direction P_1OP_2 is considered positive [see Fig. 3] then we have

$$\eta(\sigma)^{+} - \eta(\sigma)^{-} = \frac{K}{g(\sigma)} \overline{\phi'}\left(\frac{1}{\sigma}\right); \sigma \text{ on } L \tag{13}$$

where

$$K = K_1 - K_2 = 1 - e^{-2i\theta}. \tag{14}$$

We now investigate the behavior of the function $\eta(\zeta)$ as ζ approaches infinity. Let N_1 and N_2 be the principal stresses at infinity and ϕ_0 be the angle between the x-axis and the direction of N_1, writing

$$\Gamma = \bar{\Gamma} = \frac{1}{4}(N_1 + N_2)$$

and

$$\Gamma' = -\frac{1}{2}(N_1 - N_2)\, e^{2i\phi_0} \tag{15}$$

we have for $|\zeta| > 1$ the following series representation for $\phi(\zeta)$ and $\psi(\zeta)$

$$\begin{aligned} \phi(\zeta) &= \Gamma A\zeta + A_1/\zeta + A_2/\zeta^2 + \cdots \\ \psi(\zeta) &= \Gamma' A\zeta + B_1/\zeta + B_2/\zeta^2 + \cdots \end{aligned} \tag{16a}$$

where A is the real constant appearing in the mapping function $\omega(\zeta)$ [see equation (1)] and A_i, B_i $(i = 1, 2, \ldots \infty)$ are complex constants. Hence as $\zeta \to \infty$

$$\eta(\zeta) \to \Gamma A\zeta^2 + A_1. \tag{16b}$$

3. THE SECTIONALLY HOLOMORPHIC FUNCTION $\eta(\zeta)$

In view of equation (11) and the extension principle (12a, b) $\eta(\zeta)$ is holomorphic in the entire plane except at the point at infinity and on the line L. More over it is continuous from the left and from the right at all points of L with the possible exception of the end points of L, i.e. P_1 and P_2. These points, however, correspond to the origin in the z-plane, where the displacements must be bounded. It is easy to show that $\phi(\zeta)$ and therefore $\eta(\zeta)$ must also be bounded as $\zeta \to P_1$ (or P_2) from the left or from the right of L and the discontinuity $F(\sigma)$ given by (see equations (13, 14))

$$F(\sigma) = \frac{K}{g(\sigma)} \overline{\phi'}(1/\sigma); \sigma \text{ on } L \tag{17}$$

must approach zero as $\sigma \to P_1$ (or P_2). The nature of these zeroes is discussed in the next section. The function $F(\sigma)$ satisfies the Hölder condition on L and with the help of (16b) the sectionally holomorphic function $\eta(\zeta)$ can be expressed as [6, 13]

$$\eta(\zeta) = \frac{1}{2\pi i} \int_L \frac{F(\sigma)}{\sigma - \zeta} d\sigma + \Gamma A\zeta^2 + A_1 \tag{18}$$

where the integral is taken from P_1 to P_2 and A_1 is yet an undetermined constant. Substitution of

$\eta(\zeta)=\zeta\phi(\zeta)$, division of both sides by ζ and subsequent differentiation after a change in the order of differentiation and integration yields

$$\phi'(\zeta)=-\frac{1}{2\pi i\zeta^2}\int_L\frac{F(\sigma)}{\sigma-\zeta}\,d\sigma+\frac{1}{2\pi i\zeta}\int_L\frac{F(\sigma)}{(\sigma-\zeta)^2}\,d\sigma+\Gamma A-\frac{A_1}{\zeta^2}. \tag{19}$$

Replacing ζ by $1/\bar{\sigma}_0$; σ_0 on L and making use of (12b) and (17) we obtain

$$\frac{\overline{g(\sigma_0)}\,\overline{F(\sigma_0)}}{\bar{K}}=-\frac{\bar{\sigma}_0^{\,2}}{2\pi i}\int_L\frac{F(\sigma)}{(\sigma-1/\bar{\sigma}_0)}\,d\sigma+\frac{\bar{\sigma}_0}{2\pi i}\int_L\frac{F(\sigma)}{(\sigma-1/\bar{\sigma}_0)^2}\,d\sigma+\Gamma A-A_1\bar{\sigma}_0^{\,2} \tag{20}$$

where $g(\sigma_0)$ is given by (9a, b). The above equation may therefore be written in the form

$$\overline{F(\sigma_0)}=\int_L M(\sigma,\sigma_0)\,F(\sigma)\,d\sigma+f_1(\sigma_0). \tag{21}$$

The kernel $M(\sigma,\sigma_0)$ is bounded and continuous on L except at the ends, i.e. when $\sigma=\sigma_0=e^{i\alpha_j}$; $j=1,2$, where it becomes unbounded because of the second integral in (20). This behavior is a characteristic of the type of zeroes of $F(\sigma)$, which influences the nature $\phi(\zeta)$ near the end points of L. We make use of equation (20) to study this behavior in the next section.

4. THE ZEROES OF $F(\sigma)$ AT THE ENDS OF L

Since $F(\sigma)=0$ at the ends of L the second integral in (20) can be written as

$$\frac{\bar{\sigma}_0}{2\pi i}\int_L\frac{F(\sigma)}{(\sigma-1/\bar{\sigma}_0)^2}\,d\sigma=\frac{\bar{\sigma}_0}{2\pi i}\int_L\frac{F'(\sigma)}{(\sigma-1/\bar{\sigma}_0)}\,d\sigma. \tag{22}$$

We now restrict our attention in the neighborhood of one of the ends say $e^{i\alpha_2}=b$ and following[13] write $F(\sigma)$ in the neighborhood of that point as

$$F(\sigma)=F_1^*(\sigma)(\sigma-b)^{1-\gamma_2}+F_2^*(\sigma)(\sigma-b)^{1-\bar{\gamma}_2} \tag{23}$$

where $\bar{\gamma}_2$ is the complex conjugate of γ_2 and $0<Re(\gamma_2)<1$. $F_1^*(\sigma)$ and $F_2^*(\sigma)$ satisfy the Hölder condition near and at b and $(\sigma-b)^{\gamma_2}$ is any definite branch which varies continuously on L. If γ_2 is real, one can take $F_2^*(\sigma)=0$. In the neighborhood of b, $F'(\sigma)$ can be written as

$$F'(\sigma)=\frac{(1-\gamma_2)\,F_1^*(\sigma)}{(\sigma-b)^{\gamma_2}}+\frac{(1-\bar{\gamma}_2)\,F_2^*(\sigma)}{(\sigma-b)^{\bar{\gamma}_2}}+F_3^*(\sigma) \tag{24a}$$

where $F_3^*(\sigma)$ satisfies the Hölder condition near b, but may be unbounded at b. However, if it is unbounded we have

$$|F_3^*(\sigma)|<\frac{C_0}{|\sigma-b|^{\epsilon_0}} \tag{24b}$$

where C_0 and ϵ_0 are real constants such that $\epsilon_0<Re(\gamma_2)$.

Next we examine the behavior of the integrals

$$\frac{1}{2\pi i}\int_L \frac{F(\sigma)}{\sigma-\zeta_0}\,\mathrm{d}\sigma$$

and

$$\frac{1}{2\pi i}\int_L \frac{F'(\sigma)\,\mathrm{d}\sigma}{\sigma-\zeta_0}$$

when ζ_0 is near $b=\mathrm{e}^{i\alpha_2}$ but not on L. Using the results in chapter 4 of Ref. [13].

$$\frac{1}{2\pi i}\int_L \frac{F(\sigma)\,\mathrm{d}\sigma}{\sigma-\zeta_0}\to 0 \tag{25}$$

as ζ_0 approaches b along any path.

$$\frac{1}{2\pi i}\int_L \frac{F'(\sigma)\,\mathrm{d}\sigma}{\sigma-\zeta_0}=-\frac{\mathrm{e}^{-\gamma_2\pi i}(1-\gamma_2)\,F_1^*(b)}{2i\sin\gamma_2\pi(\zeta_0-b)^{\gamma_2}}-\frac{\mathrm{e}^{-\bar{\gamma}_2\pi i}(1-\bar{\gamma}_2)\,F_2^*(b)}{2i\sin\bar{\gamma}_2\pi(\zeta_0-b)^{\bar{\gamma}_2}}+\Phi_0(\zeta_0) \tag{26a}$$

where $\Phi_0(\zeta_0)$ may be bounded or unbounded as $\zeta_0\to b$. However, if it is unbounded we can write

$$|\Phi_0(\zeta_0)|<\frac{C_1}{|\zeta_0-b|^{\epsilon_1}} \tag{26b}$$

where C_1 and ϵ_1 are real constant such that $\epsilon_1<Re(\gamma_2)$.

Substitution of (23) and (9a) in the left hand side of (20) yields the following expression when σ_0 is on L and in the neighborhood of $b=\mathrm{e}^{i\alpha_2}$.

$$\frac{\overline{g(\sigma_0)F(\sigma_0)}}{\bar{K}}=\frac{\lambda_2\mathrm{e}^{-i\alpha_2}}{\bar{K}}\left[\left\{\frac{\overline{F_1^*(\sigma_0)}}{(\sigma_0-b)^{\gamma_2}}\right\}+\left\{\frac{\overline{F_2^*(\sigma_0)}}{(\sigma_0-b)^{\bar{\gamma}_2}}\right\}\right]+F_3(\sigma_0) \tag{27}$$

where

$$F_3(\sigma_0)\to 0\qquad \text{as}\qquad \sigma_0\to b.$$

If we now take $\sigma_0=R.\mathrm{e}^{i\alpha_2}$ where R is in the neighborhood of 1 and $\zeta_0=1/\bar{\sigma}_0=\mathrm{e}^{i\alpha_2}/R$ we have

$$\begin{aligned}(\sigma_0-b)^{\gamma_2}&=(1-R)^{\gamma_2}\,\mathrm{e}^{i(\pi+\alpha_2)\gamma_2}\\ \overline{(\sigma_0-b)^{\gamma_2}}&=(1-R)^{\bar{\gamma}_2}\,\mathrm{e}^{-i(\pi+\alpha_2)\bar{\gamma}_2}\end{aligned} \tag{28}$$

and

$$(\zeta_0-b)^{\gamma_2}=\frac{(1-R)^{\gamma_2}}{R^{\gamma_2}}\,\mathrm{e}^{i\alpha_2\gamma_2}$$

Substituting (25–28) in (20) and equating like singularities of the form $(1-R)^{\gamma_2}$ as $R \to 1$ in the two sides of the equation

$$\frac{(1-\gamma_2)\,F_1^{**}(b)}{2i\sin\gamma_2\pi}+\frac{\lambda_2\overline{F_2^{**}(b)}}{\bar{K}}=0 \tag{29a}$$

where K is given by (14),

$$F_1^{**}(b)=F_1^{*}(b)\,e^{-i(\pi+\alpha_2)\gamma_2}$$

and

$$F_2^{**}(b)=F_2^{*}(b)\,e^{-i(\pi+\alpha_2)\bar{\gamma}_2}. \tag{29b}$$

Similarly consideration of like singularities of the form $(1-R)^{\bar{\gamma}_2}$ as $R\to 1$ yields

$$\frac{(1-\bar{\gamma}_2)\,F_2^{**}(b)}{2i\sin\bar{\gamma}_2\pi}+\frac{\lambda_2\overline{F_1^{**}(b)}}{\bar{K}}=0. \tag{30}$$

Considering the two homogeneous equations (29a, 30) and noting that $|K|=2\sin\pi\lambda_2$ we can obtain the following transcendental equation for the determination of γ_2.

$$(1-\gamma_2)\sin\pi\lambda_2=\pm\lambda_2\sin\gamma_2\pi. \tag{31}$$

It may be noted that if γ_2 is a solution (31) $\overline{\gamma_2}$ is also a root.

In case γ_2 is real we take $F_2^*(b)=F_2^{**}(b)=0$ and obtain the following equation by considering singularities of the form $(1-R)^{\gamma_2}$ as $R\to 1$

$$\frac{(1-\gamma_2)\,F_1^{**}(b)}{2i\sin\gamma_2\pi}+\frac{\lambda_2\overline{F_1^{**}(b)}}{\bar{K}}=0. \tag{32}$$

If we now write $F_1^{**}(b)=F_4(b)+iF_5(b)$ and separate the real and imaginary parts of (32) after substituting $\bar{K}=1-e^{i2\pi\lambda_2}$ we obtain the following two homogeneous equations.

$$\begin{aligned}&[(1-\gamma_2)(1-\cos 2\pi\lambda_2)]F_4(b)+[2\lambda_2\sin\gamma_2\pi+(1-\gamma_2)\sin 2\pi\lambda_2]F_5(b)=0\\&[(1-\gamma_2)\sin 2\pi\lambda_2-2\lambda_2\sin\gamma_2\pi]F_4(b)-[(1-\gamma_2)(1-\cos 2\pi\lambda_2)]F_5(b)=0\end{aligned} \tag{33}$$

which yield the same transcendental equation (31) for determining γ_2.

By restricting our attention in the neighborhood of the end $e^{i\alpha_1}=a$ of L, if we write $F(\sigma)$ in the form (23) where b and γ_2 are replaced by a and γ_1 respectively, and follow the procedure which has been outlined above, we obtain the following equation for γ_1

$$(1-\gamma_1)\sin\pi\lambda_1=\pm\lambda_1\sin\gamma_1\pi. \tag{34}$$

Although we have obtained (31) and (34) subject to the condition $0<Re(\gamma_j)<1$; $j=1,2$, the above procedure can be readily extended for a wider range of values of γ_j and in particular when $Re(\gamma_j)<0$. The possibility that $Re(\gamma_j)>1$ is excluded, since the displacements have to be bounded at the origin in the z-plane. If we substitute $1-\gamma_j=\lambda_j\delta_j$; $j=1,2$ in (31, 34) we have

$$\lambda_j\delta_j \sin(\pi\lambda_j) = \pm\lambda_j \sin(\pi\lambda_j\delta_j); \qquad j=1,2. \tag{35}$$

The above transcendental equation was obtained by Williams [8] who considered displacement field of the form $r_0^{\delta_j} f(\theta_0)$ $(Re(\delta_j)>0)$ in a wedge; r_0, θ_0 is a polar co-ordinate system with the origin at the apex and the surfaces $\theta_0=0$ and $\theta_0=\pi\lambda_j$ of the wedge are free of stresses. With the help of equations (1, 6, 19, 22, 26, 35) it is easy to show that the stress fields in the vicinity of the origin in the z-plane, i.e. near $\zeta_j=e^{i\alpha_j}$; $j=1,2$, are similar to that considered in [8]. This similarity should be obvious from physical considerations. Williams also discussed the nature of the roots of (35). From his discussions we can conclude that if $1<\lambda_2<2$, i.e. $0<\theta<\pi$ (see Fig. 2 and eqn. (2)) there exists at least one root δ_2(or γ_2) such that

$$0<Re(\delta_2)<1 \tag{36}$$

or

$$1-\lambda_2<Re(\gamma_2)<1$$

which yields a stress singularity at the re-entrant corner at $z=0$.

5. A SYSTEM OF INTEGRAL EQUATIONS AND NUMERICAL SOLUTION

The function $F(\sigma)$ has to be obtained by solving the equation (20) which contains an unknown constant A_1. To determine this constant we investigate the behavior of $\eta(\zeta)$ as $\zeta\to 0^+$. With the help of (9a, 16, 12b) it may be shown that in the neighborhood of $\zeta=0$

$$\frac{1}{g(\zeta)} = -1+(\lambda_1 e^{-i\alpha_1}+\lambda_2 e^{-i\alpha_2})\,\zeta + 0(\zeta^2)$$

$$\overline{\phi'}(1/\zeta) = \bar{\Gamma} A - 0(\zeta^2) \tag{37}$$

and

$$\zeta\bar{\psi}(1/\zeta) = \bar{\Gamma}' A + 0(\zeta^2).$$

Hence (12*a*, 10) *yield*

$$\eta(0)^+ = -\bar{\Gamma} A - \overline{\Gamma'} A. \tag{38a}$$

Use of (18) and the Plemelj formulae for the corner point $\zeta=0$ (see Appendix 2 of Ref. [13]) gives us

$$\eta(0)^+ = \frac{\alpha_2-\alpha_1}{2\pi} F(0) + \frac{1}{2\pi i}\int_L \frac{F(\sigma)}{\sigma}\,d\sigma + A_1 \tag{38b}$$

where Cauchy Principal value of the integral is considered, i.e.

$$\frac{1}{2\pi i}\int_L \frac{F(\sigma)}{\sigma}\,d\sigma = \frac{1}{2\pi i}\int_L \frac{F(\sigma)-F(0)}{\sigma}\,d\sigma \tag{39}$$

since by the choice of the branch of the logarithmic function $\log(e^{i\alpha_2}/e^{i\alpha_1}) = -i[2\pi - (\alpha_2 - \alpha_1)]$. Now, since $\Gamma = \bar{\Gamma}$, (17) and (37) yield

$$F(\sigma) = -K\Gamma A + K\Gamma A(\lambda_1 e^{-i\alpha_1} + \lambda_2 e^{-i\alpha_2})\sigma + 0(\sigma^2) \tag{40}$$

and

$$F(0) = -K\Gamma A.$$

Equating right hand sides of (38a; 38b) and making use of (39, 40) we obtain

$$A_1 = AA_0 - \frac{1}{2\pi i}\int_L \frac{F(\sigma) - F(0)}{\sigma}\,d\sigma \tag{41a}$$

where

$$A_0 = -\Gamma - \overline{\Gamma'} + \frac{\alpha_2 - \alpha_1}{2\pi}K\Gamma \tag{41b}$$

K being given by (14).

Substitution of (41a) in (18) and a little manipulation yields

$$\zeta\phi(\zeta) = \frac{\zeta}{2\pi i}\int_L \frac{f(\sigma)}{\sigma - \zeta}\,d\sigma - \frac{K\Gamma A}{2\pi i}\left(\log\frac{\zeta - e^{i\alpha_2}}{\zeta} - \log\frac{\zeta - e^{i\alpha_1}}{\zeta}\right) + \Gamma A\zeta^2 + AA_0 \tag{42a}$$

where

$$f(\sigma) = \frac{F(\sigma) - F(0)}{\sigma} \tag{42b}$$

and

$$\log\left(\frac{\zeta - e^{i\alpha_j}}{\zeta}\right) = \log r_0 + i\theta_0 \tag{42c}$$

when

$$\frac{\zeta - e^{i\alpha_j}}{\zeta} = r_0 e^{i\theta_0} \tag{42d}$$

θ_0 being assumed lie between $-\pi$ and π. We now introduce two complex valued functions $H_1(r)$ and $H_2(r)$ of real variable r, $0 \leq r \leq 1$ such that

$$H_j(r) = \frac{1}{KA}[e^{i\alpha_j}f(re^{i\alpha_j}) - K\Gamma A]; \qquad j = 1, 2. \tag{43a}$$

From (40, 42b) and the condition $F(e^{i\alpha_j}) = 0$, $j = 1, 2$ we have

$$H_j(0) = \Gamma[e^{i\alpha_j}(\lambda_1 e^{-i\alpha_1} + \lambda_2 e^{-i\alpha_2}) - 1] \tag{43b}$$

and

$$H_j(1) = 0. \tag{43c}$$

From (43a) we have

$$f(re^{i\alpha_j}) = KA\, e^{-i\alpha_j}[H_j(r) + \Gamma]; \qquad j = 1, 2. \tag{43d}$$

Writing the integral in (42a) as a difference of two integrals, one over $OP_2(\sigma = re^{i\alpha_2})$ and the other over $OP_1(\sigma = re^{i\alpha_1})$ and substituting (43d) we can obtain an expression for $\phi(\zeta)$. Differentiation of this expression with respect to ζ (after a change of the order of differentiation and integration) yields

$$\frac{\phi'(\zeta)}{A} = \frac{K}{2\pi i\zeta^2}\left[\int_0^1 \frac{H_2(r)\,dr}{\left(\frac{re^{i\alpha_2}}{\zeta} - 1\right)^2} - \int_0^1 \frac{H_1(r)\,dr}{\left(\frac{re^{i\alpha_1}}{\zeta} - 1\right)^2} + \Gamma\left(\log\frac{\zeta - e^{i\alpha_2}}{\zeta} - \log\frac{\zeta - e^{i\alpha_1}}{\zeta}\right)\right] + \Gamma - \frac{A_0}{\zeta^2} \tag{44}$$

where the logarithms are evaluated according to (42c, d).
If we now take

$$\sigma_{0k} = Re^{i\alpha_k}; \qquad k = 1, 2 \tag{45}$$

from (17, 12b, 42b, 43b) we have

$$\frac{\phi'(1/\bar{\sigma}_{0k})}{A} = \overline{g(\sigma_{0k})}\,[R\overline{H_k(R)} + (R-1)\,\Gamma] \tag{46}$$

where $g(\sigma_{0k})$ is given by (9b).

Replacing ζ by $1/\overline{\sigma_{0k}} = e^{i\alpha_k}/R$ in (44) and equating the right hand side of the resulting equation with that of (46) we obtain, after a little algebraic manipulation, the following set of equations.

$$-h_k(R)\overline{H_k(R)} = f_k(R)\left[\sum_{j=1}^{2}\int_0^1 L_{kj}(r, R)\, H_j(r)\, dr + a_k(R)\right] + b_k(R) + \Gamma\, h_k(R) + \frac{A_0}{K} d_k(R); \quad k = 1, 2 \tag{47a}$$

where

$$\begin{aligned}
Kh_k(R) &= (Re^{i\beta_1} - e^{i\alpha_k})(Re^{i\beta_2} - e^{i\alpha_k}); \qquad k = 1, 2\\
f_1(R) &= \overline{f_2(R)} = \frac{R}{2\pi i}(Rp - 1)(R - 1)\\
a_1(R) &= \overline{a_2(R)} = \Gamma[\log(1 - Rp) - \log(1 - R)]\\
Kb_1(R) &= \Gamma e^{i\alpha_1}[\lambda_1 e^{i\alpha_1}(Rp - 1) + \lambda_2 e^{i\alpha_2}(R - 1)]\\
Kb_2(R) &= \Gamma\, e^{i\alpha_2}[\lambda_1 e^{i\alpha_1}(R - 1) + \lambda_2 e^{i\alpha_2}(R\bar{p} - 1)]\\
d_1(R) &= \overline{d_2(R)} = -2\pi i\, f_1(R)\\
L_{11}(r, R) &= L_{22}(r, R) = -\frac{1}{(rR - 1)^2}\\
L_{12}(r, R) &= \overline{L_{21}(r, R)} = \frac{1}{(rRp - 1)^2}
\end{aligned} \tag{47b}$$

In (47a, b)

$$p = e^{i(\alpha_2-\alpha_1)}, \tag{47c}$$

K and A_0 are given by (14) and (41b) respectively, and the logarithm in the expression for $a_i(R)$ is to be computed according to (42c, d).

The system of equations (47a) is more suitable for numerical computation than (20) or (21) and to convert (47a) to a discrete system we can make use of a quadrature formula of the form

$$\int_0^1 w(r)\,dr = \sum_{l=0}^{N+1} S_l\, w(r_l) \tag{48}$$

where the interval [0, 1] is divided into $(N+1)$ divisions, $r_l = l/(N+1)$ and S_l is the weight for lth term in the sum. Since $H_j(1) = 0$; $j = 1, 2$ and $H_j(0)$ are given by (43b) we can write the following discrete system for (47a)

$$-h_k(R_m)\overline{H_k(R_m)} = f_k(R_m)\left[\sum_{j=1}^{2}\sum_{l=1}^{N} S_l L_{kj}(r_l, R_m) H_j(r_l)\right] + f_k(R_m)[a_k(R_m) + e_k] + b_k(R_m)$$
$$+ h_k(R_m) + \frac{A_0}{K} d_k(R_m); \qquad k = 1, 2,\ m = 1, 2, \ldots N \tag{49}$$

where

$$R_m = \frac{m}{N+1}$$

and

$$e_1 = -e_2 = \Gamma\, S_0[\lambda_2 - \lambda_1 - \lambda_2\bar{p} + \lambda_1 p], \tag{50}$$

p being given by (47c). It may be noted that although L_{11} and L_{22} [eqn. (47b)] are unbounded when $r = R = 1$, $L_{kj}(r_l, R_m)$ is always bounded since l and m are never equal to $N+1$. It may be mentioned here that numerical solutions of integral equations with kernels which are unbounded at an end point have been attempted in the past (see for example [14]) by techniques similar to the one followed here.

Equation (49) is easily converted into a linear system of $4N$ equations for $4N$ real unknowns which can be solved on a digital computer. For brevity we omit those details here. After the solution is obtained the following version of (44) can be made use of to obtain $\phi'(\zeta)$ when ζ does not lie on L.

$$\frac{\phi'(\zeta)}{A} = \frac{K}{2\pi i\zeta^2}\left[\sum_{l=1}^{N} \frac{s_l H_2(r_l)}{\left(\frac{r_l e^{i\alpha_2}}{\zeta} - 1\right)^2} - \sum_{l=1}^{N} \frac{s_l H_1(r_l)}{\left(\frac{r_l e^{i\alpha_1}}{\zeta} - 1\right)^2}\right.$$
$$\left. + \left(\log\frac{\zeta - e^{i\alpha_2}}{\zeta} - \log\frac{\zeta - e^{i\alpha_1}}{\zeta}\right) + e_1\right] + \Gamma - \frac{A_0}{\zeta^2} \tag{51}$$

where e_1, A_0 and K are given by (50), (41b) and (14), respectively and the logarithms are evaluated according to (42c, d).

6. RESULTS AND SOME OBSERVATIONS

The cracktips in the z plane correspond to the points $Q_j(t_j = e^{i\beta_j}; j = 1, 2)$ on the unit circle in the ζ-plane (Fig. 3). If we introduce a local polar co-ordinate system r_0, θ_0 in the z-plane with the origin at the crack tip such that $\theta_0 = \pm\pi$ are the surfaces of the crack then in the conventional notation of Fracture Mechanics

$$\sigma_x + \sigma_y = Re\left\{K_c\left(\frac{2}{\pi r_0}\right)^{1/2} e^{-i\theta_0/2}\right\} + 0(r_0^{1/2}) \tag{52a}$$

where K_c is the complex stress intensity factor defined as

$$K_c = K_{\rm I} - iK_{\rm II}. \tag{52b}$$

In (52b) $K_{\rm I}$ and $K_{\rm II}$ are the stress intensity factors for opening (I) and shearing (II) mode, respectively.

In our formulation $\sigma_x + \sigma_y$ is given by the first of equations (6). Since we have assumed that the branch cut for the mapping function $\omega(\zeta)$ is inside the circle $|\zeta| = 1$ it is permissible to write a power series expansion of $\omega(\zeta)$ in the neighborhoods of $\zeta = t_j = e^{i\beta_j}$; $j = 1, 2$. With the help of this expansion and equations (6, 52a) it can be shown that the stress intensity factors K_c^j; $j = 1, 2$ at the tips are (see [11] and [15])

$$K_c^j = \frac{2\phi'(t_j)}{\{\pi\, e^{iv_j}\omega''(t_j)\}^{1/2}}; \qquad j = 1, 2 \tag{53a}$$

where

$$v_1 = 0$$
$$v_2 = \pi - \theta$$

$$\omega''(t_1) = \frac{1 - e^{i(\beta_2 - \beta_1)}}{(e^{i\beta_1} - e^{i\alpha_1})(e^{i\beta_1} - e^{i\alpha_2})} \tag{53b}$$

and

$$\omega''(t_2) = \frac{[1 - e^{i(\beta_1 - \beta_2)}]r_2^* e^{i(\pi - \theta)}}{(e^{i\beta_2} - e^{i\alpha_1})(e^{i\beta_2} - e^{i\alpha_2})} \tag{53c}$$

r_2^* and θ being the length and orientation of the branch, respectively (Fig. 2). It is necessary to compute the square root of the complex quantity $C = r_0 e^{i\theta_0}$ appearing in (53a) as $r_0^{1/2}\, e^{i\theta_0/2}$ where θ_0 lies between $-\pi$ and π. After $\phi'(t_j)$ are computed with the help of (51), the stress intensity factors $K_{\rm I}$ and $K_{\rm II}$ at each tip are easily obtained with the help of (53a) and (52b). Figures 4 and 5 show their variation with r_2^* and θ when $\Gamma' = 2\Gamma = 0{\cdot}5$; i.e. for a uniform unit tensile stress perpendicular to the main crack at infinity. Figures 6 and 7 give the values of $K_{\rm I}$ and $K_{\rm II}$ at the two tips for a uniform shear stress at infinity, i.e. $\Gamma = 0$, $\Gamma' = i$. In the Figures (4–7) r_2^* is plotted on a lograithmic scale since it is varied between 0·001 to 1·0. θ is varied from 15° to 90° at an interval of 15°. For $\theta = 0°$ we have the classical case of a straight crack of length larger than unity.

Trapezoidal rule with equal divisions was employed for the quadrature formula (48). For $r_2^* > 0{\cdot}01$ a value of $N = 20$ was sufficient to obtain the stress intensity factors accurate up to 3

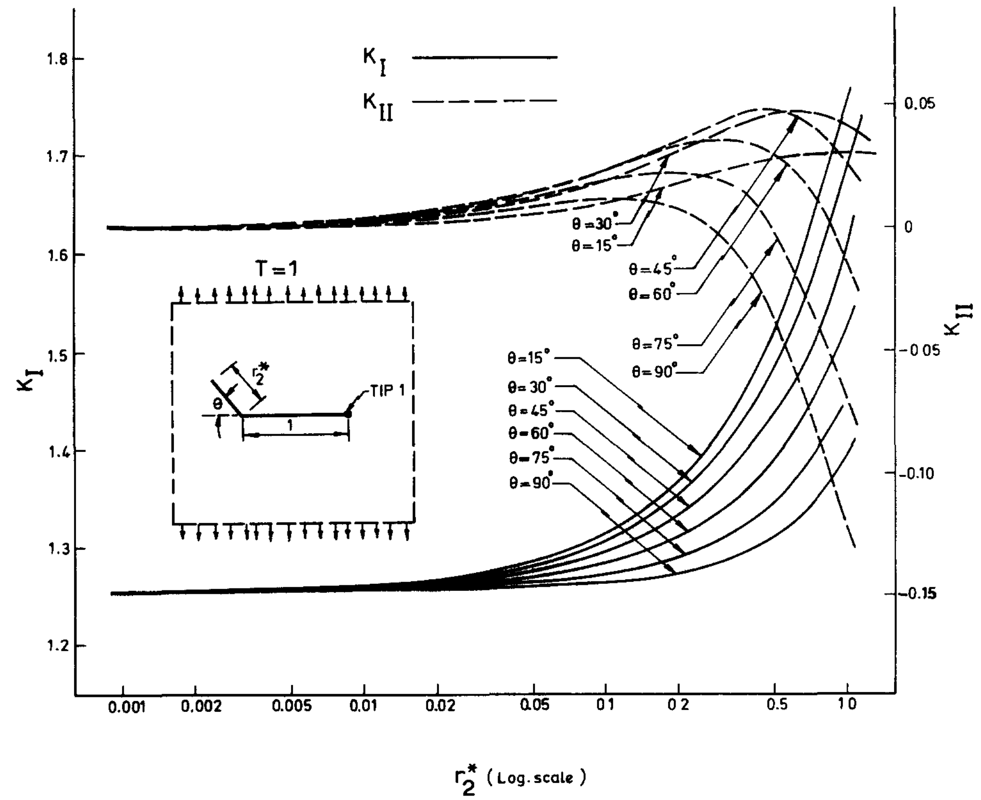

Fig. 4. Stress intensity factors at tip 1 for uniform tensile stress perpendicular to main crack at infinity.

decimal places. For smaller values of r_2^* a maximum value of $N = 30$ was chosen. It was however, necessary to put more points near the end $r = 1$ to obtain the desired accuracy.

As expected for small values of r_2^* the intensity factors at the tip of the main crack (Figs. 4, 6) are practically equal to those at the tip of a straight crack in an infinite sheet. At the tip of the branch (Figs. 5, 7) the stress intensity factors vary quite smoothly for small values of r_2^*, i.e. for r_2^* of the order of 10^{-3}. However, in general they are not close to the results obtained in [11, 12] and [9]. Although it has been suggested that the results obtained in [11, 12] are good for small values of r_2^*, no measure has been specified regarding its smallness. It is not worthwhile to try to obtain numerically the stress intensity factors for values of r_2^* less than 0·001 by the technique proposed in this study, since we expect difficulties in the numerical solution when α_1 and α_2 become too close to each other. Therefore, to make a proper comparison of the results of [11, 12, 9] with those of the present formulation, it is necessary to obtain some asymptotic solutions of the integral equations presented here for small values of r_2^*. It is hoped that such asymptotic solutions will be taken up in a future study.

Wieselmann[16] used a polynomial approximation of the mapping function $\omega(\zeta)$ and attempted to obtain the stress intensity factors at the tips of the crack configuration same as that considered here. In [16] $\phi(\zeta)$ is expressed in the form of a power series and solutions are obtained only for a few cases. It is of interest to compare these results [16] with ours (see Table 1).

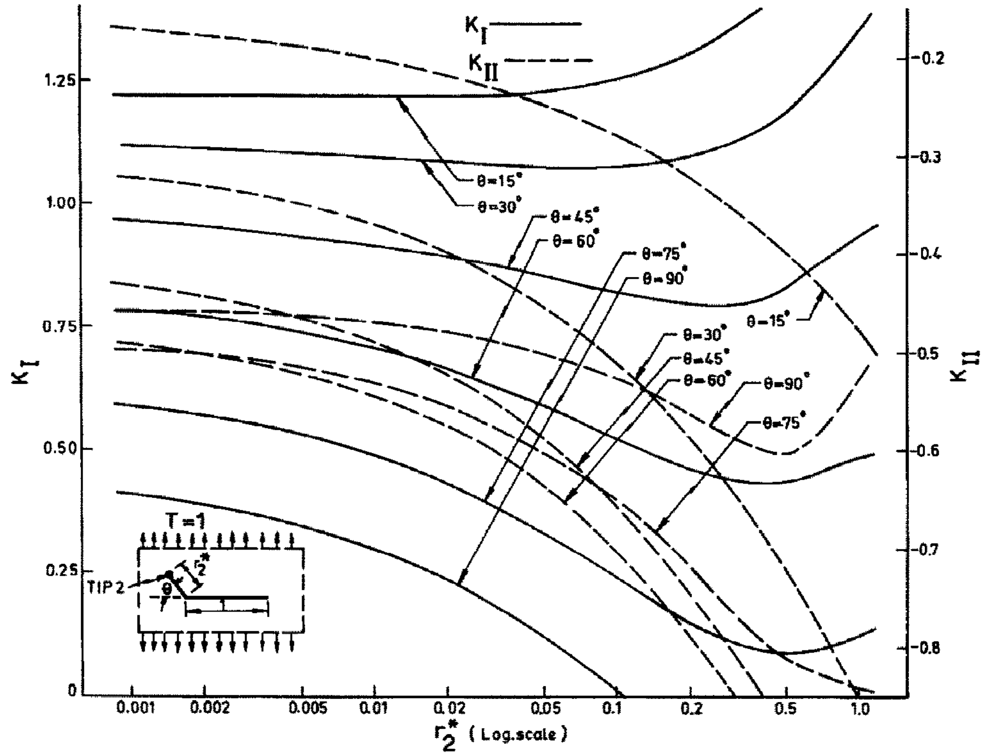

Fig. 5. Stress intensity factors at tip 2 for uniform tensile stress perpendicular to main crack at infinity.

Table 1

		K_I		K_{II}	
r_2^*	θ	Ref. [16]	Present study	Ref. [16]	Present study
0·005	45°	0·927	0·939	−0·476	−0·465
	90°	0·351	0·346	−0·451	−0·466

The above values are for the case of uniform tension perpendicular to the main crack at infinity. In the polynomial approximation technique all corners are smoothened out, but the characteristics of the cracktips are retained. In our solution no such smoothening is necessary and we have shown the existence of the stress singularity at the re-entrant corner where the two arms of the crack meet, although no attempt was made to evaluate the strength of the local singular field. Considering this fact, the differences between the values reported in [16] and the results of the present study are not significant.

Bowie and Freese [17] also attempted to obtain the stress intensity factors by a modified mapping-collocation technique. Their results are in agreement with those shown in Figs. 4 and 5. Some problems of branched cracks have been also considered by Palaniswamy (Ph. D. Thesis, California Institute of Technology, 1972). It does not seem possible however, to compare his results directly with those presented here. It may be noted that if we consider a crack

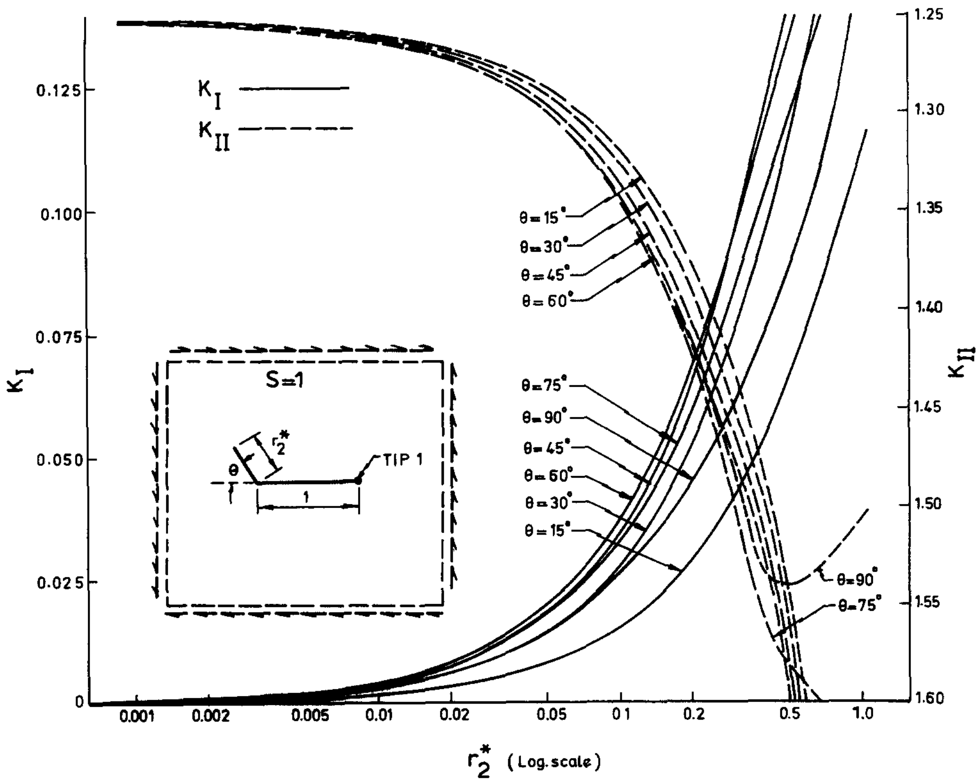

Fig. 6. Stress intensity factors at tip 1 for uniform shear stress at infinity.

configuration with $r_2^* = 1$ subjected to some particular types of traction at infinity the two cracktips may experience the same loading conditions. One such case may be obtained from the results of this study. K_I and K_{II} for $r_2^* = 1$ at the two tips are listed in the following table, since some of the values are not available from Figs. 4–7.

Table 2 ($r_2^* = 1$)

	θ	K_I^1	K_{II}^1	K_I^2	K_{II}^2
$T = 1$	15°	1·7512	0·0287	1·6619	−0·4777
Uniform tension	30°	1·6930	0·0407	1·3573	−0·8528
perpendicular to	45°	1·6127	0·0261	0·9322	−1·0499
main crack at	60°	1·5283	−0·0145	0·4865	−1·0392
infinity	75°	1·4547	−0·0701	0·1203	−0·8429
	90°	1·3984	−0·1230	−0·0921	−0·5269
$S = 1$	15°	0·1115	1·7808	0·7778	1·5706
Uniform shear	30°	0·1981	1·7974	1·3610	1·0160
stress at	45°	0·2454	1·8001	1·6064	0·2475
infinity	60°	0·2557	1·7628	1·4585	−0·5460
	75°	0·2470	1·6664	0·9619	−1·1770
	90°	0·2460	1·5072	0·2460	−1·5072

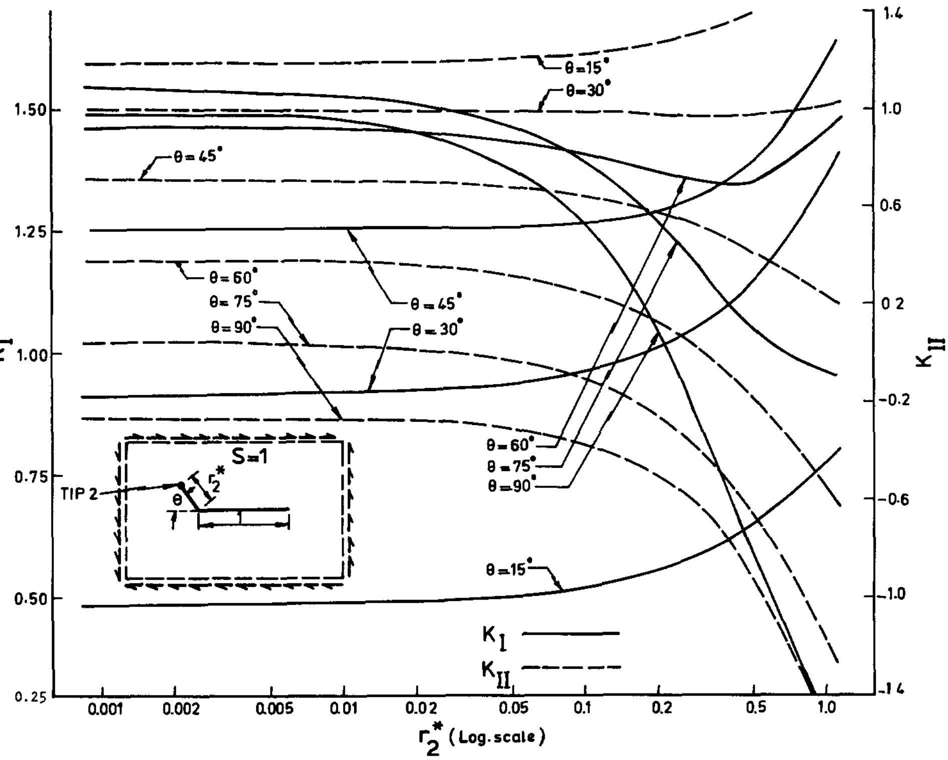

Fig. 7. Stress intensity factors at tip 2 for uniform shear stress at infinity.

The stress intensity factors due to the simultaneous application of $T = 1$ and $S = 0{\cdot}5 \tan \theta$ may be computed from the above Table and it may be seen that $K_c^1 = \overline{K_c^2}$, where K_c is the complex stress intensity factor and the superscripts indicate the tips 1 and 2. The identity also holds for the particular case $S = 1$, $\theta = 90°$ for obvious reasons. From the results reported in this study it is an easy matter to evaluate the strain energy release rates at each tip, since this rate is a known function of the stress intensity factors. However, these values may not be of much use since the branched crack considered here will not in general, extend in the direction of existing branches.

Acknowledgements—The author is thankful to Dr. J. I. Bluhm, Head, Mechanics Research Laboratory, AMMRC and to the Army Materials and Mechanics Research Center, Watertown, Massachusetts for various helps received during the progress of this work. Thanks are also due to National Research Council for the award of the Research Associateship. The author wishes to express his sincere appreciation to Messrs. O. L. Bowie, T. P. Rich, C. E. Freese and P. Tracy for suggestions and help in various stages of this work.

REFERENCES

1. H. Schardin, Velocity Effects in Fracture, in *Fracture*, edited by B. L. Averbach *et al.*, pp. 297–330. M. I. T. Press, Cambridge and Wiley, New York (1959).
2. H. Kolsky and D. Rader, Stress Waves and Fracture, in *Fracture*, edited by H. Liebowitz, Vol. VI, pp. 533–568. Academic Press, New York, (1968).
3. B. Paul, Macroscopic Criteria for Plastic Flow and Brittle Fracture, in *Fracture*, edited by H. Liebowitz, Vol. II, pp. 315–496. Academic Press, New York (1968).
4. A. A. Griffith, The Theory of Rupture, in *Proc. 1st Int. Cong. Applied Mechanics*, pp. 55–63. Delft (1924).
5. F. Erdogan and G. C. Sih, On the Crack Extension in Plates under plane Loading and Transverse Shear, *J. Basic Eng.* **85**, 519 (1963).

6. N. I. Muskhelishvili, *Some Basic Problems of the Mathematical Theory of Elasticity.* Noordhoff, Groningen (1963).
7. C. Darwin, Some Conformal Transformations Involving Elliptic Functions, *Phil. Mag.* **41**, 1 (1950).
8. M. L. Williams, Stress Singularities Resulting from Various Boundary conditions in Angular Corners of Plates in Extension, *J. Appl. Mech.* **19**; Trans. ASME **74**, 526 (1952).
9. M. A. Hussain, S. L. Pu and G. Underwood, Private Communication, Stress Instensity Factors and Strain Energy Release Rates under Mixed Mode Loading conditions, Benet Research and Engineering Laboratories, U. S. Army Watervliet Arsenal, Watervliet, N.Y., 12189, U.S.A. (1973).
10. V. V. Panasyuk, L. T. Brezhnitsky and S. Ye. Kovchik, On the Development of Arbitrarily Oriented Rectilinear Crack in Plate Under Tension, *Prikl. Mekh.* **1**, No. 2 (1965).
11. H. Andersson, Stress Intensity Factors at the Tips of a Star-shaped Contour in an Infinite Tensile Sheet, *J. Mech. Phys. Solids* **17**, 405 (1969).
12. H. Andersson, Erratum on [11], *J. Mech. Phys. Solids* **18**, 437 (1970).
13. N. I. Muskhelisvili, *Singular Integral Equations.* Wolters Noordhoff, Groningen (1958).
14. N. J. Freeman and L. M. Keer, Torsion of a cylindrical Rod Welded to an Elastic Half Space, *J. Appl. Mech.* **34**; *Trans. ASME* **89**, 687 (1967).
15. O. L. Bowie, Rectangular Tensile Sheet with Edge Cracks, *J. Appl. Mech.* **31**, 208 (1964).
16. P. A. Wieselmann, Doctoral Dissertation, Massachusetts Institute of Technology, Cambridge, Massachusetts (1969).
17. O. L. Bowie and C. E. Freese, Private Communication, Mechanics Research Laboratory, Army Materials and Mechanics Research Center, Watertown, Massachusetts, 02172, U.S.A. (1973).